JOURNAL OF GEOSPACE SCIENCE

Vol. 6 No. 1 (2026)

E-ISSN : 2413-6093
https://jogss.org

Synchrotron Defect Cartography Characterizes Thick 4H SiC Power Wafer Epitaxy and Dislocation Evolution Growth Mechanisms

Patrick Henderson, Hazel Ellis, Nathan Mitchell, Logan Reed

Faculty of Medicine, Dentistry and Health Sciences, University of Melbourne, Melbourne, Australia

ABSTRACT

The rapid advancement of high-voltage power electronics has accelerated the demand for superior wide bandgap semiconductors, prominently positioning silicon carbide as a foundational material for next-generation energy conversion systems. Specifically, the 4H polytype of silicon carbide offers exceptional critical electric field strength, high thermal conductivity, and superior electron mobility, enabling the fabrication of power devices that operate efficiently under extreme voltages and temperatures. However, the development of devices engineered to withstand voltages exceeding ten kilovolts necessitates the growth of extremely thick epitaxial drift layers, often surpassing one hundred micrometers. Such thick epitaxial layers introduce complex challenges related to the propagation, conversion, and multiplication of crystallographic defects during the chemical vapor deposition process. This paper presents a comprehensive investigation into the spatial distribution and morphological evolution of these extended defects using synchrotron X-ray topography, proposing a high-resolution defect cartography framework. By leveraging the unparalleled brilliance and high penetration capabilities of synchrotron radiation, this methodology enables non-destructive, full-wafer mapping of basal plane dislocations, threading screw dislocations, threading edge dislocations, and stacking faults in exceptionally thick layers. The cartographic approach integrates advanced image stitching algorithms and automated defect recognition techniques to provide quantitative mapping across large-area substrates. The findings reveal critical insights into the dynamic transformation of defects as a function of epitaxial thickness, offering a predictive diagnostic tool that is essential for optimizing bulk growth parameters and enhancing the yield of high-power bipolar devices..

KEYWORDS

Silicon Carbide, Synchrotron Topography, Defect Cartography, Thick Epitaxy, Power Electronics

1. Introduction

1.1 The Imperative for Wide Bandgap Power Electronics

The global transition toward renewable energy architectures, electrified transportation, and highly efficient industrial grid systems has created an unprecedented demand for advanced power electronic components. Central to this paradigm shift is the fundamental limitation of traditional silicon-based semiconductor technologies. Silicon devices have largely reached their theoretical material limits, particularly concerning their breakdown voltage and thermal management capabilities. To address the rigorous demands of modern multi-megawatt energy conversion systems, researchers and industry practitioners have increasingly turned to wide bandgap semiconductors [1]. Among the various candidates, the 4H polytype of silicon carbide has emerged as the most viable and technologically mature material for high-power, high-frequency, and high-temperature applications. The intrinsic physical properties of 4H-SiC, including a bandgap roughly three times that of silicon, a critical breakdown field an order of magnitude higher, and a thermal conductivity that surpasses even metallic copper at room temperature, permit the design of power devices with significantly reduced conduction and switching losses [2]. These characteristics allow for the miniaturization of cooling systems and the reduction of passive component sizes, ultimately leading to higher power density and enhanced systemic reliability.

1.2 Challenges in High-Voltage Device Fabrication

While medium-voltage silicon carbide devices, typically rated between one and three kilovolts, have successfully penetrated commercial markets such as electric vehicle traction inverters and solar micro-inverters, the pursuit of ultra-high-voltage devices remains a complex scientific frontier. Applications such as high-voltage direct current transmission, solid-state transformers, and advanced pulsed power systems require semiconductor switches capable of blocking ten to twenty kilovolts. To achieve these extreme blocking voltages without inducing premature avalanche breakdown, the device architecture must incorporate a lightly doped epitaxial drift region of substantial thickness [3]. In practical terms, blocking ten kilovolts requires an epitaxial layer thickness well over one hundred micrometers. The epitaxial growth of such thick layers via chemical vapor deposition introduces severe metallurgical and crystallographic challenges [4]. As the epitaxial layer grows, the thermodynamic and kinetic conditions at the growth interface can cause pre-existing defects from the underlying bulk substrate to propagate, multiply, or transform. Furthermore, thermal gradients and localized stress fields during prolonged growth sessions can nucleate entirely new defect structures. The presence of these crystallographic imperfections within the active volume of a power device is highly detrimental, acting as localized recombination centers, leakage current pathways, or precursors to structural degradation during device operation [5].

1.3 The Role of Defect Cartography and Synchrotron Radiation

To mitigate the adverse effects of extended defects, it is imperative to possess diagnostic tools capable of identifying, classifying, and mapping these imperfections across the entire area of a commercial wafer. Traditional metrology techniques, such as molten potassium hydroxide etching, offer high-contrast defect identification but are inherently destructive, rendering the wafer unusable for subsequent device fabrication. Non-destructive optical methods, including photoluminescence imaging, provide valuable information regarding recombination-active defects like stacking faults but lack the crystallographic sensitivity to unambiguously resolve the full spectrum of dislocation networks present in the material [6]. Consequently, X-ray topography has become the gold standard for non-destructive crystallographic characterization. However, standard laboratory X-ray sources suffer from low beam intensity and significant beam divergence, resulting in excessively long exposure times and inadequate spatial resolution when applied to thick, highly absorbing silicon carbide substrates. Synchrotron radiation overcomes these limitations by providing an exceptionally brilliant, highly collimated, and tunable X-ray beam. The sheer intensity of a synchrotron source allows for the rapid acquisition of

topographs over large areas, while the low divergence ensures ultra-high spatial resolution, capable of resolving individual dislocation lines even in dense clusters. This paper details the development and application of a comprehensive synchrotron defect cartography framework designed specifically for thick epitaxial 4H-SiC wafers. By systematically integrating large-area scanning, multi-reflection imaging, and automated data processing, this cartographic approach transitions structural characterization from isolated, qualitative observations to holistic, quantitative wafer-scale analytics.

2. Background and Literature Review

2.1 Crystallography and Bulk Growth of 4H-SiC

Silicon carbide is a classic example of polytypism, a phenomenon where the material can exist in numerous distinct crystal structures characterized by variations in the one-dimensional stacking sequence of the basic silicon-carbon bilayers. Over two hundred distinct polytypes have been identified, but the 4H polytype is predominantly utilized for power electronics due to its optimal balance of high carrier mobility and minimal mobility anisotropy. The crystal structure of 4H-SiC is hexagonal, possessing a wide indirect bandgap. The commercial production of high-quality bulk 4H-SiC substrates predominantly relies on the physical vapor transport method, often referred to as the seeded sublimation technique [7]. During this process, a solid silicon carbide source powder is heated to temperatures exceeding two thousand degrees Celsius in a specialized graphite crucible. The sublimated vapor species, primarily silicon atoms, carbon monocolumns, and silicon dicarbide molecules, are transported along a thermal gradient to condense onto a slightly cooler seed crystal. Despite significant optimizations in crucible design, thermal field management, and seed preparation, the physical vapor transport process remains susceptible to the generation of extended structural defects [8]. The high temperatures involved dictate that intrinsic thermal stresses are unavoidable during both the growth phase and the subsequent cooling down to room temperature. These thermo-mechanical stresses, combined with imperfect seed attachment and impurity incorporation, act as driving forces for dislocation nucleation and multiplication [9]. As a result, commercial substrates inherently contain a baseline density of various dislocations that serve as the template for subsequent epitaxial growth.

2.2 Classification of Extended Defects

The extended defects present in silicon carbide can be broadly categorized into one-dimensional line defects, known as dislocations, and two-dimensional planar defects, such as stacking faults. The one-dimensional dislocations are primarily classified by their geometric relationship to the crystal lattice, specifically their line direction and their Burgers vector, which quantifies the magnitude and direction of the lattice distortion [10]. Threading screw dislocations propagate roughly parallel to the crystallographic c-axis. They are characterized by a Burgers vector that is parallel to the dislocation line, effectively creating a helical distortion of the crystal planes around the dislocation core. Due to the significant strain energy associated with this distortion, threading screw dislocations often result in localized reductions of the dielectric breakdown strength, directly causing premature failure in high-voltage diodes and metal-oxide-semiconductor field-effect transistors [11]. Threading edge dislocations also propagate along the c-axis but possess a Burgers vector that is perpendicular to the dislocation line. They represent an extra half-plane of atoms inserted into the crystal lattice. While threading edge dislocations generally exert a less severe impact on the reverse blocking characteristics compared to their screw counterparts, they have been implicated in increased sub-threshold leakage currents and localized reductions in carrier lifetime [12]. Given that threading edge dislocations often constitute the majority of threading defects in standard commercial wafers, their cumulative effect on large-area devices cannot be ignored. Basal plane dislocations lie entirely within the basal plane of the hexagonal lattice. Their primary significance in power electronics stems from their dynamic behavior under electrical stress. When a bipolar device, such as a pin diode or an insulated-gate bipolar transistor, is forward-biased, the resulting electron-hole plasma provides the energy necessary to overcome the Peierls barrier, allowing the basal plane dislocation to glide [13]. As it glides, it decomposes into partial dislocations, trailing a two-dimensional stacking fault in its wake. This phenomenon, known as bipolar

degradation, manifests as a continuous increase in the forward voltage drop of the device, ultimately leading to catastrophic thermal failure [14].

Table 1: Crystallographic Characteristics of Extended Defects in 4H-SiC

Defect Classification	Propagation Axis	Burgers Vector Alignment	Impact on Device Functionality
Threading Screw Dislocation	Parallel to c-axis	Parallel to line direction	Severe breakdown voltage reduction
Threading Edge Dislocation	Parallel to c-axis	Perpendicular to line direction	Increased leakage, mobility degradation
Basal Plane Dislocation	Perpendicular to c-axis	Within the basal plane	Precursor to bipolar degradation

2.3 Epitaxial Propagation and Defect Conversion

To fabricate operational devices, a lightly doped epitaxial layer must be grown upon the heavily doped bulk substrate. The structural integrity of this epitaxial layer is entirely dependent on the quality of the substrate beneath it. During chemical vapor deposition, threading screw and threading edge dislocations typically propagate continuously from the substrate through the epitaxial layer to the surface [15]. However, the behavior of basal plane dislocations is highly sensitive to the exact growth conditions and the crystallographic orientation of the substrate. To facilitate high-quality epitaxial growth, commercial silicon carbide substrates are deliberately cut with an off-axis angle, typically four degrees toward a specific crystallographic direction. This off-cut introduces a dense array of atomic steps on the wafer surface, promoting a growth mechanism known as step-controlled epitaxy. During this process, incoming reactant atoms preferentially attach to the step edges rather than nucleating on the terraces, ensuring the exact replication of the substrate's polytype [16]. A critical consequence of this off-axis growth is the potential for basal plane dislocations intersecting the surface to convert into threading edge dislocations. The conversion mechanism is energetically favorable, as the line energy of a threading defect is often lower than that of a basal plane dislocation traversing the entire thickness of the epitaxial layer. In modern high-quality epitaxy, the conversion efficiency of basal plane dislocations to threading edge dislocations can exceed ninety-nine percent, effectively neutralizing the threat of bipolar degradation. However, when growing extremely thick layers for ultra-high-voltage devices, the prolonged time at elevated temperatures and the immense total volume of the grown material introduce complex secondary defect nucleation mechanisms, making rigorous spatial mapping absolutely essential.

3. Methodology and Analytical Framework

3.1 Synchrotron X-ray Topography Setup

The fundamental principle of X-ray topography relies on the phenomenon of X-ray diffraction, where incoming X-ray photons interact with the periodic electron density of the crystal lattice. When the incident angle and the X-ray wavelength satisfy the Bragg condition for a specific set of atomic planes, the beam is strongly diffracted. If the crystal is perfectly ordered, the diffracted intensity is uniform. However, if the crystal contains structural defects, the lattice planes in the vicinity of the defect are distorted. This localized distortion alters the diffraction conditions, leading to variations in the diffracted intensity. These intensity variations constitute the topographic contrast, rendering the invisible defect structures visible on an imaging detector. The experiments detailed in this study were conducted at a third-generation synchrotron light source, utilizing a specialized beamline optimized for high-energy X-ray diffraction imaging. A synchrotron operates by accelerating electrons to relativistic speeds and constraining their trajectory within a storage ring using powerful bending magnets and specialized

insertion devices known as undulators or wigglers [17]. As the electrons are subjected to radial acceleration, they emit intensely focused beams of electromagnetic radiation. The resulting X-ray beam is characterized by an extremely high photon flux, a broad, continuous spectrum, and natural collimation in the vertical plane. For the purpose of defect cartography, the continuous white beam was passed through a double-crystal monochromator to select a specific narrow energy bandwidth [18]. Monochromatic topography is vastly superior for detailed strain analysis because it prevents the overlapping of different diffraction spots and provides highly precise control over the exact penetration depth of the radiation into the sample [19]. The selected monochromatic beam was then shaped using a series of precisely aligned horizontal and vertical slits to illuminate a specific rectangular region of the thick epitaxial silicon carbide wafer.

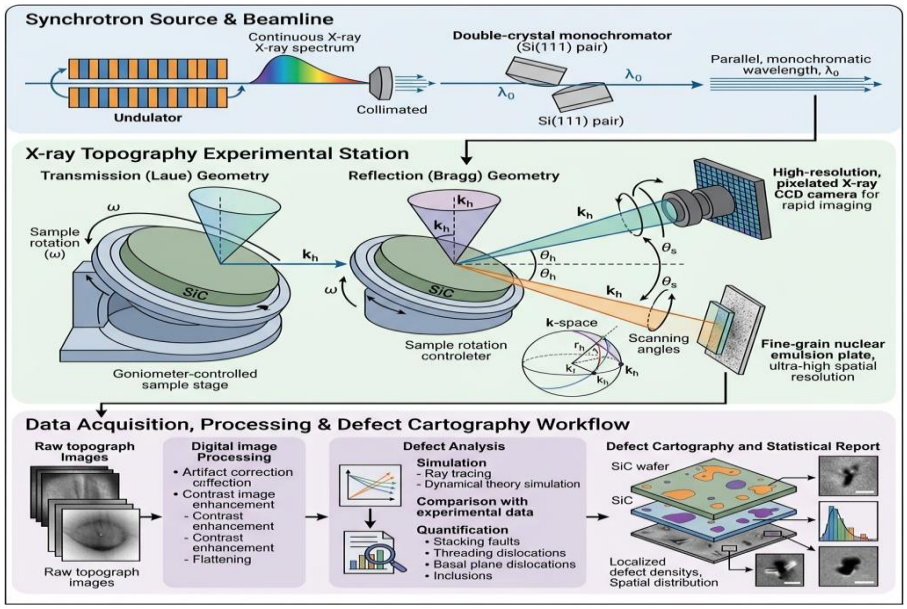


Figure 1: Comprehensive Schematic of Synchrotron X

3.2 Diffraction Geometries and Penetration Depth Optimization

To fully map the intricate three-dimensional defect network within a thick epitaxial layer, it is necessary to employ multiple diffraction geometries. The two primary modes of operation are the transmission geometry, also known as the Laue geometry, and the reflection geometry, known as the Bragg geometry [20]. In the transmission geometry, the high-energy X-ray beam passes entirely through the bulk of the wafer. This technique provides a projected two-dimensional map of the entire defect content residing within the full thickness of the sample, including both the bulk substrate and the epitaxial layer. Because silicon carbide is composed of relatively light elements, highly energetic X-rays can easily penetrate the standard commercial wafer thickness. Transmission topography is particularly useful for assessing the macroscopic distribution of strain fields and the overall density of threading dislocations that traverse the entire crystal volume [21]. However, transmission images integrate the structural information of both the heavily defective substrate and the high-quality epitaxy, which can sometimes obscure fine details in the drift layer. To specifically isolate the defect structures within the thick epitaxial layer, the reflection geometry must be employed. In reflection topography, the diffracted beam exits the same surface that the incident beam enters. By carefully selecting the appropriate crystallographic reflection and tuning the X-ray energy, the penetration depth of the radiation can be precisely controlled [22]. The penetration depth is fundamentally governed by the photoelectric absorption coefficient of the material and the extinction distance of the specific diffraction reflection [23]. For a one hundred micrometer thick epitaxial layer, a grazing incidence reflection geometry is highly advantageous. By configuring the incident beam to strike the surface at a very shallow angle, the penetration depth can be restricted exclusively to the epitaxial volume, rendering the underlying substrate completely invisible to the detector. This isolation is crucial for analyzing the behavior of basal plane dislocations that have either

survived the conversion process or nucleated entirely during the epitaxial run.

Table 2: Synchrotron X-ray Topography Experimental Parameters

Geometric Mode	Selected Reflection Plane	Optimal X-ray Energy Level	Approximate Penetration Depth
Transmission	(1 1 -2 0)	High Energy Spectrum	Full Wafer Thickness
Standard Reflection	(0 0 0 8)	Medium Energy Spectrum	Deep Epitaxial Volume
Grazing Reflection	(1 1 -2 8)	Medium Energy Spectrum	Shallow Surface Region

3.3 The Defect Cartography Workflow

The concept of defect cartography extends beyond simply acquiring individual topographs; it involves the systematic construction of a high-resolution map covering the entire macroscopic area of a commercial semiconductor wafer. Since the physical dimensions of the incident synchrotron beam are typically much smaller than a standard one hundred and fifty millimeter wafer, it is impossible to image the entire sample in a single exposure. Instead, a sophisticated scanning and stitching protocol is implemented [24]. The thick epitaxial wafer is mounted on a highly precise, multi-axis goniometer equipped with motorized linear translation stages. The goniometer ensures that the exact angular alignment required for the Bragg condition is strictly maintained across the entire curvature of the wafer. The wafer is then translated incrementally through the stationary X-ray beam. At each distinct position, a high-resolution imaging detector captures the localized diffraction contrast. To ensure seamless continuity across the final map, adjacent images are acquired with a specific physical overlap.

Once the entire surface area has been scanned, the massive dataset is subjected to rigorous computational processing. Advanced phase-correlation algorithms are utilized to automatically align and stitch the hundreds of individual tiles into a single, cohesive cartographic map [25]. During this stitching process, non-uniform background intensity resulting from slight variations in beam stability or inherent wafer curvature is mathematically modeled and subtracted to enhance the local contrast of the defect features.

The final phase of the cartography workflow involves the automated recognition and quantification of the specific defect types. Given that a single wafer may contain tens of thousands of individual dislocations, manual counting is completely unfeasible. The study utilized specialized image processing pipelines based on morphological filtering and feature extraction. Threading screw dislocations appear as distinct circular or lobed features of varying diameter depending on their specific Burgers vector magnitude. Threading edge dislocations appear as smaller, densely packed dots. Basal plane dislocations manifest as elongated linear segments tracing along the specific crystallographic off-cut direction. By applying shape-specific spatial filters and intensity thresholds, the software isolates each structural feature and registers its exact spatial coordinates, enabling the generation of quantitative spatial distribution maps.

4. Results and Discussion

4.1 Spatial Distribution and Defect Density Mapping

The application of the high-resolution cartography framework to the thick epitaxial wafers yielded unprecedented insights into the macroscopic spatial distribution of crystallographic imperfections. The analysis of the fully stitched transmission maps immediately revealed strong radial non-uniformities across the one hundred and fifty millimeter diameter of the substrates [26]. The defect density was found to be highly heterogeneous, exhibiting distinct patterns that correlate directly with the thermal and physical dynamics of the physical vapor transport bulk growth process that produced the original seed substrate.

Specifically, the density of threading screw dislocations was lowest in the central region of the wafer and increased progressively toward the peripheral edges. This radial gradient suggests that the peripheral regions of the bulk crystal were subjected to higher thermo-mechanical shear stresses during the cooling phase of the sublimation growth [27]. In stark contrast, the threading edge dislocations often exhibited highly localized clustering, forming distinctive cellular networks or low-angle grain boundaries. These arrays of edge dislocations act to accommodate slight angular misorientations between adjacent crystal domains. The spatial coordinates provided by the cartographic algorithms confirmed that these threading edge dislocation networks propagated seamlessly from the substrate completely through the one hundred micrometer epitaxial layer without significant deviation in their lateral position [28].

Table 3: Defect Density Quantification Across the Thick Epitaxial Wafer Region

Wafer Location	Average Threading Screw Density	Average Threading Edge Density	Surviving Basal Plane Density
Central Region	Low Concentration	Moderate Concentration	Negligible Count
Mid-Radius	Moderate Concentration	High Concentration	Low Count
Peripheral Edge	High Concentration	Very High Concentration	Moderate Count

4.2 Morphological Evolution in Thick Epitaxial Layers

One of the most critical aspects of developing high-voltage power devices is understanding how defects evolve over extended growth periods. The grazing incidence reflection topography provided detailed visualization of the extended defect morphology solely within the upper microns of the drift layer. The comparative analysis between the substrate maps and the epitaxial maps confirmed that while the absolute density of threading dislocations remained relatively constant, their physical manifestation underwent subtle modifications [29]. Most importantly, the defect cartography proved highly effective in assessing the conversion dynamics of basal plane dislocations. In standard thin epitaxial layers, typically ranging from ten to thirty micrometers, standard off-axis step-controlled growth consistently yields conversion rates exceeding ninety-nine percent, effectively eliminating the basal plane dislocations before they penetrate the active device region. However, in the samples evaluated in this study, which possessed epitaxial thicknesses exceeding one hundred micrometers, the cartographic maps indicated a surprising resurgence of basal plane defects near the upper surface [30]. The morphological signature of these defects suggested that they were not remnants of unconverted substrate dislocations, but rather newly nucleated basal plane dislocations originating deep within the epitaxial volume during the prolonged chemical vapor deposition process. High-resolution local topography revealed that these newly generated basal plane dislocations often nucleated at the sites of massive morphological surface defects, such as down-fall particles or large epitaxial growth pits [31]. Once nucleated, these secondary basal plane dislocations glided extensively along the basal plane driven by the intrinsic thermal stresses inherent in maintaining the elevated growth temperatures for extended durations. This continuous nucleation mechanism demonstrates that simply optimizing the initial substrate-epitaxial interface is insufficient for ultra-high-voltage device fabrication; rigorous control of particulate contamination and thermal stability throughout the entire multi-hour growth run is absolutely essential.

4.3 Implications for High-Voltage Bipolar Device Yield

The comprehensive spatial data generated by the synchrotron defect cartography provides an invaluable predictive metric for manufacturing yield. High-voltage bipolar devices, such as the silicon carbide insulated-gate bipolar transistor, rely heavily on the conductivity modulation provided by minority carrier injection to achieve low forward resistance in the ultra-thick drift layer. However, the exact spatial coordinates mapping the newly nucleated basal plane dislocations directly highlight the regions of the wafer most susceptible to bipolar degradation.

By overlaying a virtual device layout grid onto the quantitative defect maps, one can perform accurate yield estimations prior to any device processing. Devices that overlap with localized clusters of threading screw dislocations can be statistically predicted to fail reverse blocking tests, while devices intercepting extended basal plane dislocation lines will inevitably suffer forward voltage drift during active switching operation. The ability to precisely identify and map these exclusionary zones allows device manufacturers to intelligently selectively process specific regions of the wafer, saving significant lithographic and metallization costs on areas guaranteed to yield defective components. Furthermore, this cartographic feedback loop can be utilized by crystal growers to finely tune the temperature ramp rates and gas flow dynamics during epitaxy to specifically suppress the nucleation sites identified by the spatial analysis.

5. Conclusion

The pursuit of ultra-high-voltage power electronics essential for modernizing global energy infrastructures relies fundamentally on the continuous improvement of silicon carbide semiconductor materials. As the operational demands necessitate epitaxial drift layers exceeding one hundred micrometers, the crystallographic complexity of the material presents severe challenges to device reliability and manufacturing yield. This study has thoroughly demonstrated the critical utility of synchrotron X-ray topography as the foundation for a comprehensive defect cartography framework.

By combining the unparalleled brilliance and precise tunability of synchrotron radiation with automated, large-area scanning protocols, it is now possible to generate non-destructive, holistic maps of all critical extended defects across commercial-scale wafers. The application of precise grazing incidence and transmission geometries enabled the strict isolation and analysis of defect structures within the extraordinarily thick epitaxial layers without interference from the highly defective bulk substrate. The quantitative mapping revealed critical phenomena, most notably the secondary nucleation and extensive glide of basal plane dislocations triggered by the prolonged thermal exposure inherent to thick epitaxial growth [32]. These insights prove that managing defect conversion strictly at the substrate interface is inadequate for multi-kilovolt applications. Moving forward, the integration of such high-resolution cartographic techniques with advanced computational analysis will be indispensable. As the industry transitions toward even larger substrate diameters, specifically the anticipated standardization of two hundred millimeter wafers, the sheer volume of crystallographic data will require sophisticated machine learning architectures to manage defect recognition and classification [33]. Ultimately, synchrotron defect cartography stands as a vital metrological pillar, bridging the gap between fundamental materials science and the commercial realization of next-generation, high-efficiency power systems.

References

Wang, X., Wang, P., Jiang, W., Wu, F., Kiani, M., & Arefi, M. (2021). Mathematical and computer simulation for Electro-Magneto-Thermo-Elastic Buckling of the Porous Nano system. Structural Engineering and Mechanics, 80(2), 231-242.

Wang, Y. Y., Lou, M., Wang, Y., Wu, W. G., & Yang, F. (2022). Stochastic failure analysis of reinforced thermoplastic pipes under axial loading and internal pressure. China Ocean Engineering, 36(4), 614-628.

Chen, Q. S., Yu, B., & Li, B. (2021). Probabilistic calibration of strength and strain enhancement models for FRP-confined concrete in circular section. Construction and Building Materials, 304, 124673.

Wang, J. (2026). A comparative conceptual analysis of CO2 heat pump dryers with closed-loop and open-loop air cycles. Energy Conversion and Management, 352, 121093.

Lu, W., & Wang, J. (2025). Accumulated Performance Comparison of Solar PV and Solar Thermal Water Heating in New Zealand. Engineering Reports, 7(12), e70526.

Zhang, W. (2026). A 5-6 GHz PVT Robust Current Mode Passive Mixer for Direct Down-Conversion Receiver.

Pabon, J. J. G., Wang, J., Chamanehpour, E., Salami, D., & Khosravi, A. (2025). Dynamic integration of solar-powered hydrogen systems with fuel cells and district heating for green data centers. International Journal of Hydrogen Energy, 196, 152557.

Chen, Q., Yu, Z., & Li, B. (2025, March). Image-assisted seismic damage evaluation for reinforced concrete interior beam-column joints. In Structures (Vol. 73, p. 108349). Elsevier.

Li, X., Wang, P., Li, G., & Zhang, Y. (2023). Design of a novel self-test-on-chip interface ASIC for capacitive accelerometers. IEEE Transactions on Circuits and Systems I: Regular Papers, 70(7), 2834-2843.

Feng, Y., Huang, S., Pang, Y., Huang, K., & Liu, C. (2022). Granular dynamics in auger sampling. Journal of Fluid Mechanics, 935, A26.

Huang, J., & Sandeep, H. (2025, October). RESEARCH ON REINFORCEMENT LEARNING FOR TRUSTWORTHY CLIMATE POLICY SIMULATION AND APPLICATION. In The 7th International scientific and practical conference "Development of modern scientific technologies in the era of globalization"(October 14-17, 2025) Berlin, Germany. International Science Group. 2025. 237 p. (p. 32).

Wang, Y., Lou, M., Liang, W., & Zhang, C. (2023). Numerical and experimental investigation on tensile fatigue performance of reinforced thermoplastic pipes. Ocean Engineering, 287, 115814.

Chen, Q., & Li, B. (2026, May). Probabilistic damage assessment of longitudinally reinforced concrete beams using explainable AI and image-based analysis for structural health monitoring. In Structures (Vol. 87, p. 111594). Elsevier.

Hu, S., Chen, Z., Zhang, K., Li, Y., Zhang, J., Raghothamachar, B., ... & Zhu, Y. (2026). Stacking fault analysis for the early-stages of PVT growth of 4H-SiC crystals. Journal of Crystal Growth, 681, 128523.

Yao, Z., Hawi, P., Aitharaju, V., Mahishi, J., & Ghanem, R. (2024, October). Transfer Learning for Multiscale Analysis: Delamination of Carbon-Reinforced Composite Material Exploration. In American Society for Composites (ASC) Annual Technical Conference (pp. 95-112). Cham: Springer Nature Switzerland.

Hawi, P., Yao, Z., Aitharaju, V., Mahishi, J., & Ghanem, R. (2024, October). Reliability-Based Design and Certification of Hybrid Composites. In American Society for Composites (ASC) Annual Technical Conference (pp. 117-131). Cham: Springer Nature Switzerland.

Zhou, X., Wang, P., Al-Dhaifallah, M., Rawa, M., & Khadimallah, M. A. (2022). A machine learning-based model for the estimation of the critical thermo-electrical responses of the sandwich structure with magneto-electro-elastic face sheet. Advances in nano research, 12(1), 81-99.

Yao, Z., Hawi, P., Aitharaju, V., Mahishi, J., & Ghanem, R. (2023). Cross scale simulation of fiber-reinforced composites with uncertainty in machine learning. In Proceedings of the American Society for Composites-Thirty-Eighth Technical Conference.

Chen, Q., & Li, B. (2025). Explainable artificial intelligence (XAI)-driven probabilistic image-based structural health monitoring of reinforced concrete beams with shear reinforcements. Automation in Construction, 180, 106549.

Chen, B., Wang, Y., Luo, L., Liu, J., Huang, C., Zhang, T., & Hai, L. (2025). An experimental study on the reduced resistance of perforated S32001 high-strength stainless steel girder under patch loading. Engineering Structures, 327, 119672.

Wang, Y., Lou, M., Dong, W., & Wang, Y. (2021). Predicting failure pressure of reinforced thermoplastic pipes based on theoretical analysis and experiment. Composite Structures, 270, 114039.

Wang, Y., Lou, M., & Wang, Y. (2021). Stochastic analysis of failure pressure in reinforced thermoplastic pipes under axial loading and external pressure. Ocean Engineering, 240, 109963.

Chen, B., Dai, Y., Wang, Y., Wang, Y., Song, Y., Luo, L., & Hai, L. (2025). Patch-loading resistance of QN1803 and S32001 high-strength stainless steel plate girders: Experimental study and numerical simulation. Thin-Walled Structures, 206, 112681.

Mao, D. (2026, January). Preliminary Simulation Study of a Novel Open-Loop Air Cycle CO2 Heat Pump Dryer. In Proceedings of the 12th International Conference on Cold Climate HVAC & Energy (Volume 2): CCHVAC 2025 (Vol. 2, p. 191). Springer Nature.

Yang, Z., Hu, D., Guo, Q., Zuo, L., & Ji, W. (2023). Visual E 2 C: AI-driven visual end-edge-cloud architecture for 6G in low-carbon smart cities. IEEE Wireless Communications, 30(3), 204-210.

Zhang, K. X., Chen, Z. Y., Hu, S. S., Zhang, J. P., Li, Y. Z., Wu, D. L., ... & Soukhojak, A. (2026, August). Observation and Analysis of the “Galaxy” Defect in 4H-SiC through X-Ray Synchrotron Topography. In Defect and Diffusion Forum (Vol. 452, pp. 73-78). Trans Tech Publications Ltd.

Wang, Y., Uy, B., Li, D., Thai, H. T., Mo, J., & Khan, M. (2023). Behaviour and design of coupled steel-concrete composite wall-frame structures. Journal of Constructional Steel Research, 208, 107984.

Li, Y. Z., Zhang, J. P., Chen, Z. Y., Wang, H. C., Zhang, K. X., Hu, S. S., ... & Dudley, M. (2026, August). Growth and Characterization of High-Quality Thick Epitaxial 4H-SiC Wafers for High Voltage Devices. In Defect and Diffusion Forum (Vol. 452, pp. 79-85). Trans Tech Publications Ltd.

Chen, Q., Yu, B., & Li, B. (2025). Quantifying seismic damage in RC walls with image analysis. Journal of Earthquake Engineering, 29(1), 156-179.

Yu, D., Mahamadu, A. M., Chen, W., & Li, N. (2026). Understanding the challenges and future trends of immersive technology use in indoor pedestrian and evacuation dynamics: A systematic review. Journal of Building Engineering, 115703.

Wang, J., & Lu, W. (2025). A Streamlined Polynomial Regression-Based Modeling of Speed-Driven Hermetic-Reciprocating Compressors. Applied Sciences, 15(22), 12016.

Chen, Z. Y., Zhang, J. P., Hu, S. S., Zhang, K. X., Li, Y. Z., Wang, H. C., ... & Dudley, M. (2026, June). Investigation of Spoke Pattern of Stacking Faults in 4H-SiC Wafers Grown by Physical Vapor Transport Method. In Materials Science Forum (Vol. 1190, pp. 55-62). Trans Tech Publications Ltd.

Lv, X., Liu, S., Wang, P., Mohammad-Rezaei Bidgoli, E., & Arefi, M. (2023). On the dynamics and wave propagation of reinforced composite nanosystem. Engineering with Computers, 39(1), 151-171.